Reprinted from Estuarine and Coastal Modeling III
Proceedings of the 3rd International Conference
Sponsored by the Waterway, Port, Coastal and Ocean Div./ASCE
September 8-10, 1993, Oak Brook, Illinois

Coastal Circulation and Sedimentation During Severe Storms

Timothy R. Keen[1,2], Scott M. Glenn[1], and Rudy L. Slingerland[3]

Abstract

Numerical hindcasts of storm flows and sedimentation during tropical cyclones in the western Gulf of Mexico, and a northeaster in the Middle Atlantic Bight, are summarized and compared. Physical causes of the differences in the hindcast flows and sedimentation are discussed. Circulation and sedimentation patterns are more uniform during the northeaster because the larger wind field associated with an extratropical cyclone matches regional coastal embayments better than the smaller, but more intense wind fields of tropical cyclones. Sedimentation is more variable during tropical cyclones and is more dependent on local coastal geometry and storm path.

Modeling Storm Sedimentation

The observed distribution of storm sediments on the Texas shelf has variously been interpreted as arising from offshore ebbing storm surge flow (Hayes, 1967), along-shelf wind driven flow (Morton, 1981), and obliquely offshore geostrophic downwelling flow (Snedden et al., 1988). The concept of downwelling geostrophic flow is supported by observations from the Middle Atlantic Bight (MAB) of North America (Swift et al., 1981; Lyne et al., 1990). In addition, observations from the Great Barrier Reef, Australia, reveal sediment resuspension on the inner shelf and onshore transport on the middle and outer shelf (Gagan et al., 1990).

[1] Institute of Marine and Coastal Sciences, Rutgers University, New Brunswick, NJ 08903.

[2] Present address: Naval Research Laboratory, Code 7320, Stennis Space Center, MS 39529.

[3] Department of Geosciences, Pennsylvania State University, University Park, PA 16802.

In an effort to understand the driving mechanisms for these different modes of storm sedimentation, a numerical model system was constructed for continental shelf water depths (Keen and Slingerland, 1993a). The original Storm Sedimentation System S^3 (Fig. 1) consists of numerical models of: 1) a cyclone wind field; 2) finite-depth storm waves; 3) three-dimensional coastal circulation; 4) the combined wave-current bottom boundary layer; 5) the entrainment and transport of sediment; and 6) conservation of mass (erosion and deposition) at the sea floor. The original formulation and operation of S^3 are discussed in Keen and Slingerland (1993a). The storm wind field is calculated at each grid point by a simple cyclone wind model based on the pressure distribution across the storm radius. The combined wave-current bed shear stresses used for calculating sediment transport in the original S^3 are computed by the suspended sediment stratification corrected bottom boundary layer model of Glenn and Grant (1987). The bed load transport rate and reference concentration used for calculating the suspended sediment profile are found from a modified Bagnold formulation (van Niekerk et al., 1992) and the suspended sediment profile is found from the Rouse equation. The bed load calculations are based on the maximum shear velocity $u_{*_{cw}}$ as defined by Grant and Madsen (1979). Erosion and deposition are calculated by bed conservation equations. If sediment transport is increasing in the flow direction (i.e., positive $u_{*_{cw}}$ gradients), erosion occurs but, if transport decreases in the flow direction (negative $u_{*_{cw}}$ gradients) deposition results. The sediment entrainment algorithm neglects cohesion, bed armoring, and grain hiding and thus over predicts entrainment of fine sediment. This problem is further discussed by Keen and Slingerland (1993a). The original version of S^3 was used in all Gulf of Mexico experiments discussed in this paper.

The bottom boundary layer model has been incorporated into the coastal circulation model in order to calculate both the combined wave-current bottom shear stresses and sediment transport while the circulation field is being computed. This coupled model has been described and evaluated by Keen and Glenn (1993a) for stratified continental shelf flow. Because of the dominance of suspended sediment transport during storms, the bed load is neglected in the coupled model. The modified Bagnold formulation for finding the reference concentration has been replaced with the algorithm contained within the bottom boundary layer model, using excess skin friction following Glenn and Grant (1987). The suspended sediment profile is thus dependent on the eddy viscosity profile in the combined wave-current boundary layer. The instantaneous reference concentration is averaged over the significant wave period and thus introduces the time-average of the instantaneous transport rate. This transport rate is slightly lower than the maximum found from $u_{*_{cw}}$. This modification has made the calculation of sediment transport consistent with the theory for computing combined wave-current shear stresses. Bed conservation is calculated in the same manner as in S^3. The coupled model was used for the MAB experiments.

Both S^3 and the coupled model are intended to simulate processes governing sedimentation on the continental shelf for water depths greater than 10 m. This

focus is based on the difficulty of resolving the shore face with spatial scales appropriate to the rest of the shelf, and the lack of sufficient understanding of sediment transport processes within the coastal zone. Because of this simplification, it is necessary to parameterize shore face erosion. This was accomplished in S^3 by matching transport out of a shoreward boundary grid point with transport into it from the landward boundary. Thus, erosion is precluded from any grid point adjacent to land. Although this is a significant simplification it was introduced to represent shore face erosion from barrier islands such as bound the Gulf of Mexico and the MAB. This boundary condition was applied to all experiments discussed below.

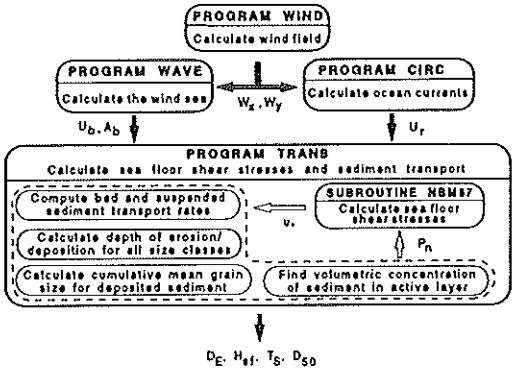

Figure 1. Schematic flow chart for the original version of S^3 (from Keen and Slingerland, 1993a). For application to the MAB, the wind stress components W_X and W_Y are found from hindcast winds, and the wave field used to compute the wave orbital speed U_b and diameter A_b has been replaced by hindcast waves. Subroutine NBM87 has been replaced by the coupled model (Keen and Glenn, 1993a), which calculates suspended sediment transport. Program TRANS solves the bed conservation equation in the new version. Output variables are depth of erosion into original sea bed D_E, sea floor height H_{sf}, thickness of deposited sediment T_S, and volumetric mean grain size of sediment D_{50}.

Storm flow and sedimentation in the western Gulf of Mexico

The original version of S^3 was used to simulate circulation and sedimentation during tropical cyclones in the western Gulf of Mexico. The evolution of the wind, wave, and circulation fields, as well as the sedimentation resulting from different initial sediment distributions, are discussed for Tropical Storm Delia in Keen and Slingerland (1993a). Peak surface currents greater than 100 cm/s first occurred near the Louisiana coast (Fig. 2a) and migrated westward while strengthening until hour 20 (Fig. 2b), when a maximum of more than 200 cm/s was located near

Galveston. At landfall (Fig. 2c) peak currents were still found at Galveston, driven by the ebbing storm surge. The coastal flow had migrated nearly 500 km westward in response to the moving storm wind field which maintained a coherent structure.

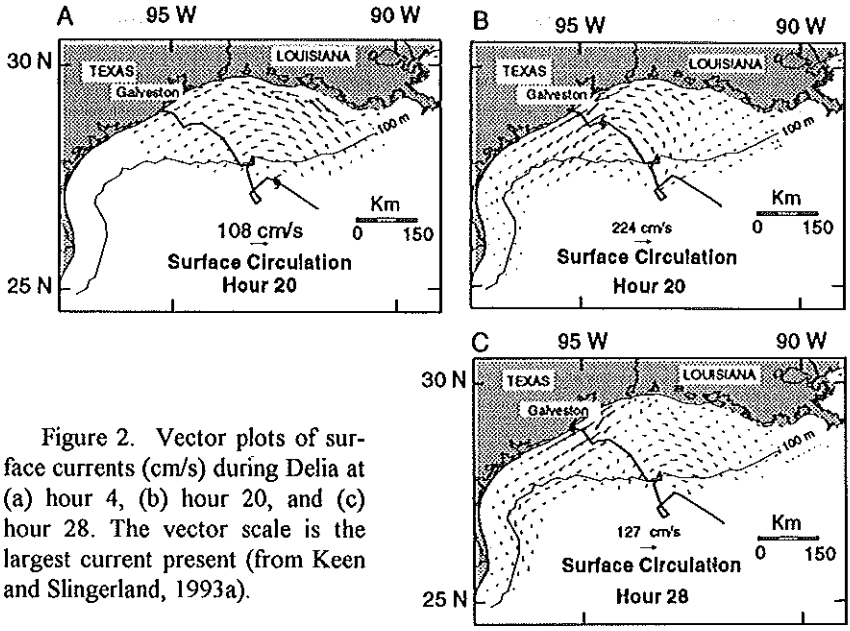

Figure 2. Vector plots of surface currents (cm/s) during Delia at (a) hour 4, (b) hour 20, and (c) hour 28. The vector scale is the largest current present (from Keen and Slingerland, 1993a).

Storm currents were greatest near the coast at hour 4, but the maximum shear velocity in the wave-current boundary layer u_{*cw} (Fig. 3a) was highest along the 20-m isobath because storm waves were larger in deeper water. Although erosion and deposition depend on transport gradients, these are frequently dependent primarily on u_{*cw} and gradients of u_{*cw} can be used to evaluate patterns of erosion and deposition. Thus at hour 20, when peak surface currents were located near Galveston, u_{*cw} (Fig. 3b) was a maximum at a depth of 30 m and large positive gradients occurred in deeper water where currents were onshore, resulting in erosion and landward transport on the outer shelf. At landfall (Fig. 3c) u_{*cw} was high near the coast, because of strong currents driven by the wind stresses and the ebbing storm surge, and on the middle shelf where storm waves were highest.

The distribution of sediments in the western Gulf of Mexico reflects coastal sources of sand along Texas, the introduction of silt and clay at the Mississippi River, and relict sand along the courses of ancient rivers. Simulating sediment transport with such a complex sediment pattern is very difficult, and previous work has shown that using a mud line, with sand on the inner shelf and mud on the outer shelf, adequately represents observed sediments for shelf-scale studies (Keen and Slingerland, 1993a).

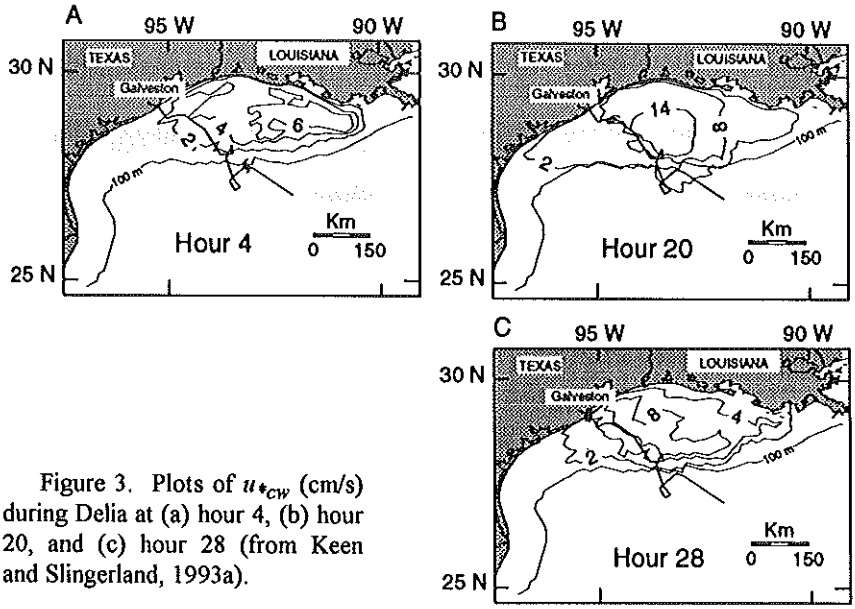

Figure 3. Plots of $u_{*_{CW}}$ (cm/s) during Delia at (a) hour 4, (b) hour 20, and (c) hour 28 (from Keen and Slingerland, 1993a).

The results discussed below for Tropical Storm Delia are from an experiment with a mud line at the 20-m isobath. The sediment distributions were composed of ten size classes from 0.0001 to 0.1 cm. The inner shelf sediment had a mean of 0.018 cm, and the outer shelf sediment had a mean of 0.0004 cm. The maximum erosion depth on the outer shelf (Fig. 4a) reflects the large positive gradients in $u_{*_{CW}}$, as fine sediment was entrained where storm waves were highest and transported both landward and along the shelf (Fig. 4b). The resulting deposit had a maximum thickness of more than 20 cm and formed an arcuate bed extending from 100 to 20 m depths. Sand was deposited landward of 20 m after being eroded from the shore face and transported across the inner shelf. The inner shelf deposit near Galveston was produced late during the storm by the offshore flow seen in Fig. 2c.

Tropical storm circulation and sedimentation in the western Gulf of Mexico were compared for several historical hurricanes by Keen and Slingerland (1993b). The discussion below focuses on Hurricane Carla because of the central role its deposit has assumed in the discussion of storm sedimentation. The surface flow field (Fig. 5a) was similar to that of Delia in the northwest Gulf, but was more extensive while being weaker. The smaller currents were the result of the lower storm surge predicted by S^3 because of the mismatch between the moving wind field and coastal geometry. However, along-shelf currents were convergent southeast of Galveston and extended south to Mexico. The storm flow also lasted longer than that for Delia, persisting for several days. The distribution of $u_{*_{CW}}$ (Fig. 5b) was much broader than for Delia, with magnitudes in excess of 4 cm/s from eastern

Louisiana to south Texas when the eye made landfall. As in Delia, u_{*cw} gradients were positive in the east and negative in the west.

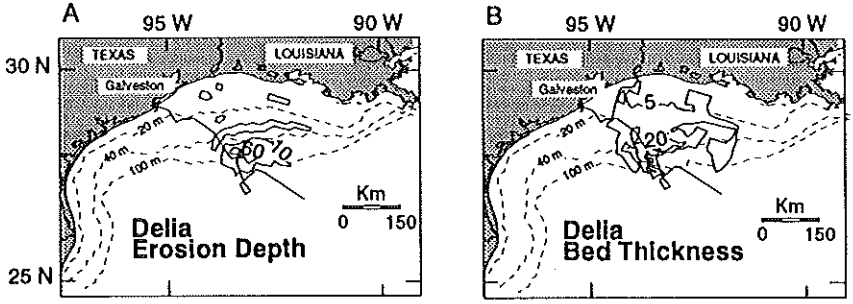

Figure 4. Plots of (a) total erosion depth (cm) and (b) total deposited sediment thickness (cm) for Delia. The initial sediment distribution consisted of fine sand landward of the 20-m isobath, and mud seaward. These results were calculated by the original version of S^3 (from Keen and Slingerland, 1993a).

The observed distribution of sediment in the western Gulf of Mexico can be reasonably represented by a mud line at a depth of 40 m, as was done by Keen and Slingerland (1993b). The deeper mud line was introduced in order to increase the volume of sand in the simulation, especially in light of the overproduction of fine sediment by S^3. Sediments were represented by 10 size classes as above. Because of the duration of storm currents and waves on the shelf, erosion (Fig. 5c) was extensive during Carla on the outer shelf of southeastern Louisiana and near the storm track, but was limited off of south Texas. Most erosion occurred during storm approach when currents in the east were higher. Erosion near Mexico, however, occurred later as the storm surge began to ebb in the south. Sand was eroded from the shore face and deposited on the inner shelf near the point of landfall (Fig. 5d). This was also a region of mixing of outer shelf mud and inner shelf sand. The pattern of deposition along the south Texas shelf was similar to that reported by Hayes (1967) and Snedden et al. (1988).

A comparison of hindcasts of Delia, Carla, and other tropical cyclones (Keen and Slingerland, 1993b) allowed several generalizations to be made for the Gulf of Mexico. Sedimentation was parallel to isobaths on the inner shelf and obliquely seaward at the coast. On the broad, shallow Louisiana shelf (Fig. 6a), separate flow and sedimentation regimes were apparent on the inner and outer shelf. Significant onshore transport occurred on the outer shelf, whereas coastal erosion supplied sand to be transported short distances offshore. Between these areas, flow and sediment transport were primarily along-shelf to the left (looking down the storm track). Where the coastline was straight and the shelf narrow (Fig. 6b), as in the southwest Gulf of Mexico, storm currents and sediment transport paths were

parallel to isobaths at all water depths. For a large embayment, such as from Galveston to Mexico (Fig. 6c), a cell developed which consisted of offshore flow in the south as well as the components for a broad shelf.

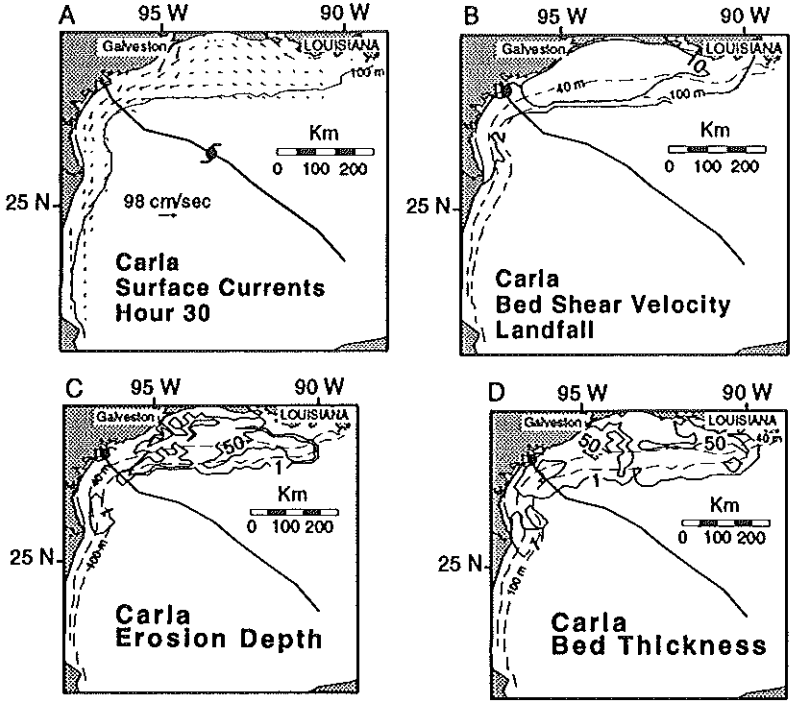

Figure 5. Results of Hurricane Carla hindcast using the original S^3. (a) Surface currents (cm/s) at hour 30. The scale vector is the largest current present. (b) Plot of $u_{*_{CW}}$ at landfall. (c) Total erosion depth (cm). (d) Total deposited sediment thickness (cm) (from Keen and Slingerland, 1993b).

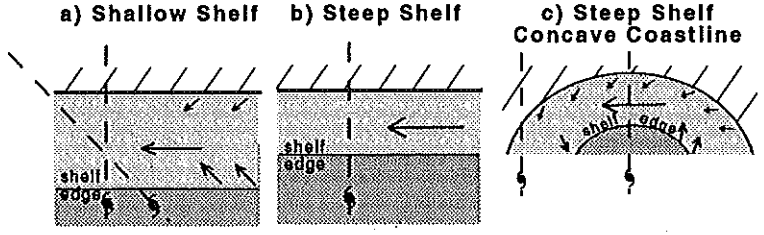

Figure 6. Schematic circulation and suspended sediment transport paths for tropical cyclones. The length of the arrows indicates the relative volume of sediment transported along each path (from Keen and Slingerland, 1993b).

Circulation during the SWADE storm

Keen and Glenn (1993a) evaluated the coupled hydrodynamic-bottom boundary layer model for extremes of stratification during upwelling and downwelling favorable winds. Cross-shelf flow was enhanced by the wave-induced increase in bottom friction, especially for strong summer stratification. Greater bottom friction increased vertical mixing, thickened the bottom boundary layer, and shifted the three-layer geostrophic flow offshore. Currents in shallow water were decreased by as much as 25% by additional drag, and the angle between surface and bottom currents increased by as much as 10° on the outer shelf. Stratification persisted for more than 12 hours in all but the shallowest water for 10 m/s winds.

The coupled model was used to hindcast circulation and sedimentation during a northeaster storm which passed over the MAB during Intense Observation Period 1 of the Surface Wave Dynamics Experiment (SWADE) in October 1990 (Keen and Glenn, 1993b). This storm has since been referred to as the SWADE storm (Weller et al., 1991). Hindcast winds and waves were made available by the SWADE group (V. Cardone and H. C. Graber, pers. com.). Details of the observed and hindcast winds and waves are discussed in Caruso et al. (1993). The storm center passed along the MAB seaward of the shelf break, and winds within the region remained constant to the southwest for approximately 24 hours before shifting offshore during the latter part of the storm. Significant wave heights and periods increased to the southwest during the storm peak and weakened after the wind changed direction because of the decreased fetch of offshore winds. Thus, vertical mixing due to the wind stress and bottom friction was limited relative to the simple case discussed by Keen and Glenn (1993a), and stratification persisted during the hindcast period. Hindcasts were completed that both included and neglected the semidiurnal M_2 and diurnal K_1 tidal components. The discussion below focuses on a hindcast that included tidal forcing, and compares results for flood (1106 EDT Oct. 26) and ebb (1718 EDT Oct. 26) tides that coincided with the storm peak.

Shelf surface currents during the flood tide (Fig. 7a) were parallel to the coast because of the balance between onshore tidal flow and Ekman drift, and opposing offshore storm surge driven flow and bottom friction. The smaller along-shelf component at the bottom (Fig. 7b) did not mask the tidal flow which has magnitudes of 10-20 cm/s, except in the south where the storm surge was larger. Along-shelf currents in the south were stronger due to the early buildup of the storm surge there and flow convergence caused by narrowing of the continental shelf. The different flow directions at the surface and bottom were possible because of persistent stratification (Keen and Glenn, 1993b). Downwelling flow, with offshore magnitudes of less than 10 cm/s, was established at this time throughout the MAB in hindcasts that did not include tides (Keen and Glenn, 1993b).

Surface currents increased slightly during the ebb tide (Fig. 7c) because the along-shelf component of the tidal flow was in the same direction as the storm-driven currents. The combined tide and storm flow in the south was stronger

because of reinforcement by the ebbing storm surge flow. Bottom currents during the ebb tide (Fig. 7d) had also increased in strength because the offshore tidal flow was superimposed on downwelling storm currents. The resulting flow on the shelf was almost directly seaward throughout the MAB.

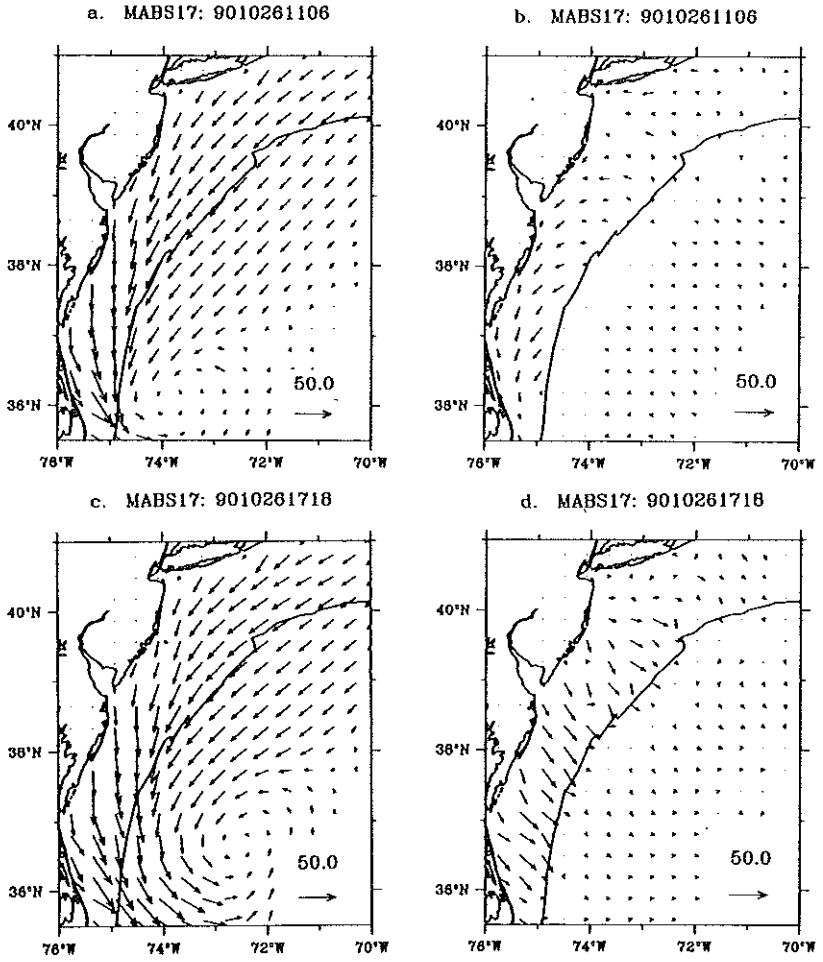

Figure 7. The calculated flow field (cm/s) for the SWADE storm (from Keen and Glenn, 1993b). (a) Surface currents during flood tide. (b) Bottom currents during flood tide. (c) Surface currents during ebb tide. (d) Bottom currents during ebb tide. The solid line offshore is the 200-m isobath.

Sedimentation during the SWADE storm

Although sediment entrainment in the coupled model, as used in the MAB study, differs from S^3 because of the use of the time-average of the suspended sediment profile, the distribution of $u_{*_{cw}}$ can be compared to that from the Gulf of Mexico because this parameter is computed in the same way. The distribution of $u_{*_{cw}}$ at 1700 EDT OCT. 26 (during the storm peak and an ebb tide) is thus presented in Fig. 8a (compare to Fig. 3). The maximum of more than 18 cm/s occurred in the south where both currents and waves were largest. Unlike the migrating pattern noted for tropical cyclones, however, this distribution did not change. The variability associated with tidal currents discussed above for the bottom flow field was not apparent in $u_{*_{cw}}$ because of the domination of instantaneous shear stresses by waves which remained high until the winds shifted offshore.

Bottom sediment within the MAB is dominated by relict sands (Knebel, 1981), and so has been simply represented in this study by one size class, very fine sand with a diameter of 0.007 cm. Although this is a simpler sediment distribution than discussed above for the Gulf of Mexico hindcasts, it is reasonable based on observed sediments and hindcasts for different distributions in the Gulf of Mexico (Keen and Slingerland, 1993a). The vertically integrated suspended sediment transport rates (volumetric transport per square cm of sea floor, cm^2/s) for flood and ebb tides during the storm peak revealed significant variability, as suggested by the bottom currents from Fig. 7. Maximum transport rates were approximately 30 cm^2/s during the flood tide (Fig. 8a), and increased to more than 160 cm^2/s in the south during the ebb tide (Fig. 8c). The highest transport was therefore seaward. After the winds shifted offshore they were in the same approximate direction as the ebb tide at 0600 EDT Oct. 27 and transport rates increased relative to the preceding flood tide, forming a pattern similar to Fig. 8c but with magnitudes 100 times smaller.

Because of the landward boundary condition, and the offshore bottom flow during the storm peak, shore face sand was transported to the middle shelf. Erosion on the shelf itself was less than 0.01 cm with local maxima of about 0.1 cm in the south. Deposition ranged from 0.05 cm near the coast to approximately 1.6 cm near Cape Hatteras (Fig. 8d), with a tongue projecting to the north on the middle shelf. The bulk of these sediments were deposited during the storm peak. Additional coastal erosion supplied sand to the middle part of the MAB and local deposition exceeded 0.3 cm on the middle shelf by the end of the hindcast period.

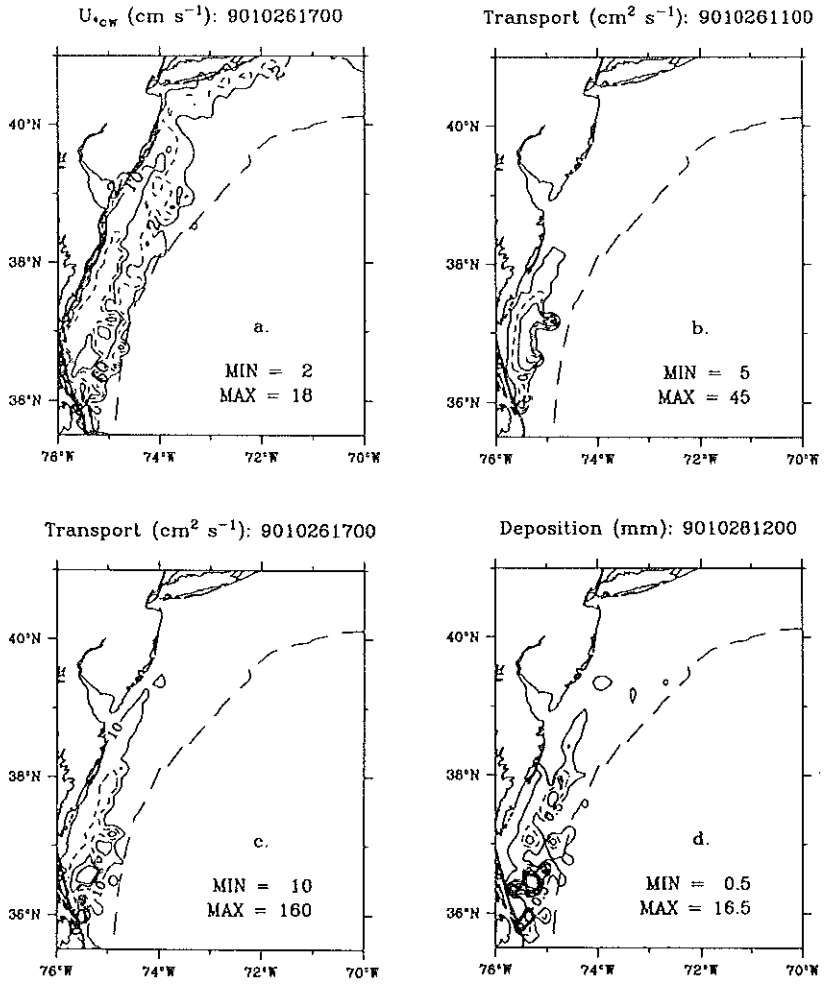

Figure 8. Hindcast sedimentation for the SWADE storm using the modified version of S^3. (a) Plot of u_{*cw} (cm/s) at the storm peak during ebb tide. The contour interval is 4 cm/s. (b) Suspended sediment transport rate (cm^2/s) at the storm peak during flood tide.. The contour interval is 10 cm^2/s. (c) Suspended sediment transport rate (cm^2/s) at the storm peak during ebb tide. The contour interval is 50 cm^2/s. (d) Total sediment deposited (mm). The contour interval is 2 mm. The solid offshore line is the 200-m isobath.

Comparison of storm sedimentation in the Gulf of Mexico and the MAB

The wind fields associated with tropical and extratropical cyclones form in response to a pressure gradient across the storm radius. This pressure gradient is larger in a tropical cyclone and produces a smaller and more intense wind field, whereas extratropical cyclones have lower gradients and form less well defined wind fields. Thus, the wind stresses are more variable as a tropical cyclone moves across the shelf before making landfall. This was especially apparent in the Gulf of Mexico wind fields which were generated by a simple cyclonic wind model. The larger size of the SWADE storm produced slower changes in the wind field, and winds remained downwelling favorable throughout much of the MAB for more than 24 hours. As the storm center moved to the northeast, winds rotated to offshore over much of the region at about the same time.

The influence of regional geometry is more apparent in the MAB because the larger size of the SWADE storm nearly matched the coastline. Strong flows persisted in the south despite periodic fluctuations in tidal flow and a change in the regional wind direction. This kind of scale matching was most apparent in the Gulf of Mexico at smaller coastal promontories such as at Galveston. This location consistently had the largest storm surge and flow in all hindcasts (Keen and Slingerland, 1993b). The larger salient at the Mexican border was only important in storms with more southerly tracks. The location of such salients partly determines the evolution of storm flows during severe storms and the full development of a coastal cell (Fig. 6c) is governed by the relationship between the storm wind field and coastal geometry (Keen and Slingerland, 1993b). Since the MAB and northwest Gulf of Mexico embayments are of similar dimensions, it is apparent that the size of extratropical cyclones allows them to fit regional coastal geometry better and thus exemplify the ideal coastal cell illustrated by Fig. 6c. The SWADE hindcasts did not reveal the up-coast end of a cell, however, because the model grid and hindcast wind and wave fields did not extend far enough seaward to allow this flow to be reproduced.

As a result of the smaller wind fields of tropical cyclones, onshore flow was common and significant quantities of sediment were transported landward. Much of this sediment was mud but sand was also transported onshore (Keen and Slingerland, 1993a). Onshore transport was minor during the SWADE storm, however, being limited to flood tides. The unavailability of fine sediments in the SWADE hindcasts also affected the results. It is notable that sediment was swept along the shelf in the Gulf by the propagating storm current system. This pattern failed to develop in the MAB.

The water column in the Gulf of Mexico study was homogeneous, and this restricted the development of downwelling flow on the shelf. Model results for 10 m/s winds (Keen and Glenn, 1993a) suggest that the water would have been well mixed even if stratification were included, at least in shallow water within the region of maximum winds. It is likely that downwelling would have been prevalent along the coast away from the strongest winds, such as to the south of Hurricane

Carla's track as suggested by Snedden et al. (1988). However, in water depths of 20 m or less, stratification would have been destroyed by even moderate wind stresses. For example, although stratification persisted in the SWADE hindcasts, downwelling was restricted to water depths greater than 20 m.

The larger wind stresses associated with the tropical cyclones produced storm surges in excess of 100 cm in different coastal areas as the storms moved across the Gulf. These storm surges were consistently greater than that from the SWADE storm and the increased pressure gradients drove larger offshore currents in shallow water near the coast. Such flows were weak during the SWADE storm and offshore flow at the coast was dominated by ebb tides.

Astronomical tides in the Gulf of Mexico are small and tidal currents are insignificant relative to storm currents within the region of storm winds, where bottom currents exceeded 50 cm/s in all hindcasts. Tidal flow contributed to the SWADE storm flow, however, causing sediment transport rates to increase when coastal downwelling coincided with ebb tide flow. An ebb tide occurred during the peak storm flow, and when ebb tides did not coincide with downwelling, sedimentation was greatly reduced.

The combination of these factors produces different sedimentation patterns during tropical and extratropical cyclones. Maximum erosion and deposition are associated with large storm waves near the storm track in tropical cyclones. Sedimentation also occurs where storm currents are large because of the storm surge and wind stresses. Sediment is also eroded at the coast where offshore flow transports shore face sediment to the inner shelf. Because of the migrating storm current system, sedimentation is widely distributed during tropical cyclones. Erosion in the MAB was primarily from the shore face and sediment was transported further offshore by combined ebb tide and downwelling currents. Some sedimentation also occurred in the south where strong currents and large waves persisted throughout the storm. Although the types of sediment and the entrainment function were different in these hindcasts, these comparisons are supported by the distribution of u_{*cw}.

Conclusion

Simulations of storm flows and sedimentation during tropical cyclones in the Gulf of Mexico suggest the existence of coastal cells, with onshore sediment transport to the right of the storm track and offshore transport to the left. Flow is to the left (looking along the storm path) between these extremes in the ideal cell. Coastal erosion occurs by offshore flow associated with geostrophic adjustment currents and storm surge ebb flows. Maximum sedimentation is predicted near the storm track on the outer shelf where storm waves are highest. Sediment transport is broadly distributed because of migration of the storm current regime with the storm eye. Because of their small size and rapid movement, tropical cyclone flows and sedimentation are dependent on local variability of the coast line.

The larger SWADE wind field matched the MAB geometry and produced a larger and more persistent flow than that of tropical cyclones, and it was modified by tidal flows of similar magnitude as the storm currents at the bottom. Resulting periodic variations in cross-shelf flow produced greater offshore sediment transport during an ebb tide which coincided with the storm peak. This sediment was primarily eroded from the shore face and erosion was minimal on the shelf. Local variability in coastal configuration was a less important factor during the SWADE storm because of the match between its wind field and the MAB.

Acknowledgments The second author was partially supported by funds from the NOAA/NURP New York Bight Center. Computer resources were furnished by the Institute of Marine and Coastal Sciences and the Cornell National Supercomputer Facility, a resource of the Cornell Theory Center, which receives major funding from the National Science Foundation and IBM Corporation, with additional support from New York State and members of its Corporate Research Institute. Contribution number 93-43 of the Institute of Marine and Coastal Sciences, Rutgers University.

References

Caruso, M. J., Graber, H. C., Jensen, R. E., and Donelan, M. A., Observations and Modelling of Winds and Waves During the Surface Wave Dynamics Experiment, Technical Report CERC-93-6. U. S. Army Corps of Engineers, 1993.

Gagan, M. K., Chivas, A. R., and Herczeg, A. L., Shelf-wide erosion, deposition, and suspended sediment transport during Cyclone Winifred, central Great Barrier Reef, Australia, Journal of Sedimentary Petrology, 60, pp. 456-470, 1990.

Glenn, S. M., and Grant, W. D., A suspended sediment stratification correction for combined wave and current flows, Journal of Geophysical Research, 92, pp. 8244-8264, 1987.

Grant, W. D., and O. S. Madsen, Combined wave and current interaction with a rough bottom, Journal of Geophysical Research, 84, 1797-1808, 1979.

Hayes, M. O., Hurricanes as geological agents: case studies of Hurricanes Carla, 1961, and Cindy, 1963, Report of Investigations No. 61, Texas Bureau of Economic Geology, 57 p. 1967.

Keen, T. R., and Slingerland, R. L., A numerical study of sediment transport and event bed genesis during Tropical Storm Delia, Journal of Geophysical Research, 98, pp. 4775-4791, 1993a.

Keen, T. R., and Slingerland, R. L., Four storm-event beds and the tropical cyclones that produced them: a numerical hindcast, Journal of Sedimentary Petrology, 63, pp. 218-232, 1993b.

Keen, T. R., and Glenn, S. M., A coupled hydrodynamic-bottom boundary layer model of Ekman flow on stratified continental shelves, Journal of Physical Oceanography, in press, 1993a.

Keen, T. R., and Glenn, S. M., A coupled hydrodynamic-bottom boundary layer model of storm and tidal flow in the Middle Atlantic Bight of North America, Journal of Physical Oceanography, in review, 1993b.

Knebel, H. J., Processes controlling the characteristics of the surficial sand sheet, U.S. Atlantic outer continental shelf, Marine Geology, 42,349-368, 1981.

Lyne, V. D., Butman, B., and Grant, W. D., Sediment movement along the U. S. east coast continental shelf, II. Modelling suspended sediment concentration and transport rate during storms, Continental Shelf Research, 10, pp. 429-460, 1990.

Morton, R. A., Formation of storm deposits by wind-forced currents in the Gulf of Mexico and the North Sea: Holocene Marine Sedimentation in the North Sea Basin, Special Publication No. 5, S. D. Nio, R. T. E. Shuttenhelm, and T. C. E. van Weering, eds., International Association of Sedimentologists, pp. 385-396, 1981.

Snedden, J. W., Nummedal, W. D., and Amos, A. F., Storm- and fair-weather combined flow on the central Texas continental shelf, Journal of Sedimentary Petrology, 58, pp. 580-595, 1988.

Swift, D. J. P, Young, R. A., Clarke, T. L., Vincent, C. E., Niedoroda, A., and Lesht, B., Sediment transport in the Middle Atlantic Bight of North America: synopsis of recent observations: Holocene Marine Sedimentation in the North Sea Basin, Special Publication No. 5, S. D. Nio, R. T. E. Shuttenhelm, and T. C. E. van Weering, eds., International Association of Sedimentologists, pp. 361-383, 1981.

van Niekerk, A., Vogel, K. R., Slingerland, R. L., and Bridge, J. S., Routing of heterogeneous size-density sediments over a movable stream bed: Model development, Journal of Hydraulic Engineering, 118, 246-262, 1992.

Weller, R. A., Donelan, M. A., Briscoe, M. G., and Huang, N. E., Riding the crest: a tale of two wave experiments, Bulletin American Meteorological Society, 72, pp. 163-183, 1991.